

## Hidden hydrophobicity impacts polymer immunogenicity

Zhefan Yuan,<sup>a</sup> Patrick McMullen,<sup>a</sup> Sijin Luozhong,<sup>a</sup> Pranab Sarker,<sup>b</sup> Chenjue Tang,<sup>a</sup> Tao Wei<sup>\*b</sup> and Shaoyi Jiang<sup>\*a</sup>

<sup>a</sup> Meinig School of Biomedical Engineering, Cornell University, Ithaca, NY 14853, USA

E-mail: sj19@cornell.edu,

<sup>b</sup> Department of Chemical Engineering, Howard University, Washington, D.C. 20059, USA

E-mail: tao.wei@howard.edu

### Materials and methods

#### Materials

Methoxypolyethylene glycol amine (mPEG-NH<sub>2</sub>, 5k and 10kDa) was purchased from Alfa Aesar. Methoxypolyethylene glycol maleimide (mPEG-maleimide, 5k and 10kDa), Poly(2-methyl-2-oxazoline) piperazine terminated (PmOX, 10kDa) and Poly(2-ethyl-2-oxazoline) piperazine terminated (PeOX, 10kDa) were obtained from Sigma-Aldrich. HO-PEG-NH<sub>2</sub> (5k and 10kDa) was purchased from Creative PEGWorks. MPEG-SH (5k Da) was purchase from Nanocs. Amine-terminated polycarboxybetaine (PCB-NH<sub>2</sub>, 10kDa) was prepared and purified according to a previous protocol.<sup>1</sup> Endotoxins in polymers used for protein conjugation were reduced to <0.1 EU/mg by either an endotoxin removal column (ThermoFisher) or Triton-114 phase separation.<sup>2</sup> L-Asparaginase (Asp) was purchased from ProSpec. Imject maleimide-activated mCKLH, N- $\alpha$ -maleimidoacet-oxysuccinimide ester (AMAS) and Traut's reagent were obtained from ThermoFisher. All chemicals were used as received unless otherwise specified.

#### Polymer solubility test

The solubility of polymers was measured by a plate-based method.<sup>3</sup> Generally, light scattering of polymer solutions (0.5mg/ml in 50mM phosphate buffer, pH=7.2) at 350 nm were recorded in the presence of two salt types (sodium chloride and ammonium sulfate) at different concentrations in 96-well UV-transparent microplates. O.D. at 350nm was plotted with respect to salt concentration to determine the change in polymer solubility.

#### Hydrophobic interaction chromatography (HIC)

HIC experiments were performed on the ÄKTA pure protein purification system (Cytiva) equipped with a butyl group functionalized HIC column (HiTrap Capto Butyl, 4.7 ml, GE health). 4M NaCl or 2M AS solution buffered with 50mM phosphates (pH 7.2) were used as high salt mobile phases and for column equilibration. 100 $\mu$ l of polymer solution (10mg/ml) in the corresponding mobile phase was loaded onto the columns. Isocratic eluent was run at 1.0 ml/min for 10min or until the complete elution of weak bounded peaks. All bounded peaks were washed out using a linear gradient eluent (10min at 1.0 ml/min, from 100% to 0% salt solution), followed by another 10min of eluent with 50mM phosphate buffer. Sample elution was monitored by UV (214nm for polymers, 254nm for protein and conjugates) and conductivity detectors.

#### Preparation of polymer KLH conjugates

Polymer-KLH conjugates were prepared according to a vendor provided protocol (ThermoFisher). Typically, amine-terminated polymers were first activated by Traut's reagent (amine/Traut's reagent: 1/2). The thiol activated polymers were purified by desalting column (Bio-rad) and then mixed with maleimide modified KLH in PBS (protein conc. 4mg/ml) and kept at 4°C overnight. Unreacted polymers and small molecular impurities were removed by extensive centrifugal filtration (MW cutoff, 100kDa). 660nm protein assay (Pierce) was used to determine KLH amount in every conjugate formulation. The corresponding unconjugated KLH was used as standard sample in the 660nm protein assay. To determine polymer density of each KLH conjugate

formulation, a PBS solution containing 5mg of KLH was buffer exchanged with DI water and re-confirmed protein content by 660nm protein assay. Then the solution was lyophilized and weighed. Weight difference and related polymer molecular weight were used to calculate the number of attached polymer chains.

### **Preparation of PCB-Asp and PEG-Asp conjugates**

Preparation of PCB-ASP and PEG-ASP conjugates were performed according to our previous report.<sup>4</sup> 10mg Asp was dissolved in 5ml pH7.4 PBS buffer and then AMAS crosslinker (2.16mg, 40mg/mL in DMSO) was added into the solution. After 1h of incubation at room temperature, activated ASP (AMAS-ASP) was concentrated 3 times by centrifugal filtration (MW cutoff, 30k). PCB-SH (200mg, 10kDa) or mPEG-SH (100mg, 5kDa) prepared by the same method mentioned above were mixed with 5mg of AMAS-Asp, respectively. The mixtures were kept shaking at 4°C overnight. Unreacted polymers and small molecular impurities were removed by extensive centrifugal filtration (MW cutoff, 100kDa). Protein contents were determined by 660nm protein assay (Pierce). Asp and Asp conjugates were further characterized by HIC mentioned above (4M NaCl to 0M NaCl, Capto butyl column). SDS-PAGE was used to characterize molecular weight and distribution of Asp and Asp conjugate formulations. Samples in reducing SDS loading buffer were loaded on a 4-12% polyacrylamide gel (Bolt Bis-Tris, ThermoFisher). Electrophoresis process was run in bis-tri buffer under 140V for 40min. Precision Plus protein unstained standards were used as molecular weight standard. All the bands were stained with SYPRO Orange (ThermoFisher) and imaged by a gel imager (ImageQuant 800, Cytiva).

### **SEC for protein conjugates**

Analytical SEC was performed on a 1260 Infinity quaternary high-performance liquid chromatography system (HPLC, Agilent Technologies) equipped with an SEC Column (Ultrasphere 1000, 7.8 mm\*300 mm, Waters). Sample profiles were monitored by a UV detector (Agilent Technologies), a multi-angle light scattering (MALS) detector (miniDAWN TREOS, Wyatt), and a differential refractive index (dRI) detector (Optilab T-rEX, Wyatt). The flow rate was set at 0.5 mL/min with the mobile phase PBS (pH 7.4) containing 0.02% sodium azide as a preservative. Lab scale high-throughput SEC was performed on an FPLC system (ÄKTA pure, Cytiva) equipped with a SEC column (Superdex 200 increase 10/300 gl, Cytiva). PBS was used as mobile phase. Isocratic eluent was run at 0.7ml/min and samples were monitored by UV signal at 254nm.

### **Animal study**

C57bl/6 mice, a widely used animal model in pharmaceutical evaluation for drugs, were chosen here to study the immunogenicity of polymer and polymer-protein conjugates.<sup>5</sup> The Institutional Animal Care and Use Committee (IACUC) of Cornell University approved all animal experiments under protocol #2020-0037. C57LB/6 mice (male, body weight 20–25 g) from Jackson Laboratories were randomized into treatment groups with a sample size of five animals per group. For polymer immunogenicity studies, mice were S.C. injected with polymer-KLH conjugates on day 1 at a dose of 2.5 mg/kg (protein amount) and boosted with another dose on day 15. All the mice were sacrificed on day 22 and serum were collected and stored at -20°C for further test. For immunogenicity studies of Asp conjugates, mice were S.C. injected with Asp or Asp conjugates at a dose of 2.5 mg/kg (protein amount) on the 1<sup>st</sup> day of every week. After 3 doses of injection, all the mice were euthanized on day 28 and blood serum were collected and stored at -20°C for further test.

### **Antibody detection by indirect ELISA**

Indirect ELISA is the main or the only widely accepted method to evaluate antibody (Ab) generation against a new antigen such as zwitterionic pCB polymer when the antigen-specific monoclonal antibody against this antigen is not available. Polymer-BSA conjugates, used in ELISA plate coatings for detecting anti-polymer Abs, were prepared with similar polymer density to reduce plate coating variations. Antigens used in anti-Asp Abs and anti-whole conjugate Abs tests were un-modified asparaginase and corresponding polymer-Asp conjugates that were injected into mice. To avoid interference from detergents, PEG based surfactants like Tween or Triton-X were excluded from solutions in the ELISA experiment. Typically, 100 µL of polymer-BSA conjugates or Asp (10 µg/mL of protein concentration) solution in 0.1 M sodium carbonate buffer (pH 9.4), was added into each well of the 96-well plates. Plates were incubated at 4 °C overnight to achieve antigen coating. After discarding antigen solutions, wells were washed five times using Tris buffered saline (TBS 1X, pH 7.4) and then filled with 200ul of blocking buffer (1% BSA in 1X TBS buffer). After incubation at room temperature for 1 h, blocking buffer was aspirated and all wells were washed by TBS buffer five times. Serial dilutions of serum samples in blocking buffer were added to the plates (100 µL/well) and the plates were incubated for 1 h at 37 °C. The plates were then washed five times with TBS buffer. Subsequently, goat anti-mouse secondary antibody HRP conjugate solution was added to the plates (100 µL/well, dilution 1:20000, ThermoFisher). After 1h of incubation at 37°C, solution was discarded, and the plates were washed five times using TBS buffer. Then, 100 µL/well of HRP substrate (1-

Step Turbo TMB, Pierce) was added. The plates were shaken for 30 min, and 50  $\mu$ L stop solution (0.2 M  $H_2SO_4$ ) was added to each well. Absorbance at 450 nm (signal) and 570 nm (background) was recorded by a microplate reader.

### Atomistic Molecular Dynamics Simulations and Free Energy Computation

Atomistic molecular dynamics simulations were performed using the GROMACS software<sup>6</sup> with the CHARMM36 force field parameters<sup>7</sup> and the TIP3P water model. The dimensions of solvation systems are around  $3.3 \times 3.3 \times 3.3$  nm<sup>3</sup> with the periodic boundary condition. For each solvation system of a chemical compound, we adopted a simulation protocol, starting with an initial energy minimization and further relaxation using the leap-frog stochastic dynamics integrator with a time step of 1.0 fs in an NVT ensemble for 5 ns and then in an NPT ensemble for 5 ns before reaching the final stage of 5 ns in another NPT ensemble to compute the solvation free energy. The cutoff distance of the neighbor searching was 1.2 nm, beyond which the long-range electrostatic interactions were computed using the particle mesh Ewald (PME) method<sup>8</sup> with a Fourier grid spacing of 0.12 nm and 6th-order interpolation. To smoothly truncate the Lennard Jones (LJ) interactions, the switching function was used starting at 1.0 nm and the cutoff distance was set to 1.2 nm. The long-range dispersion correction on energy and pressure was also applied. For the thermostat at 300 K, the inverse friction constant was set to 1.0 ps. For an NPT ensemble, the method of Parrinello-Rahman was used to maintain the pressure at 1 bar.

Hydration free energies  $\Delta G$  were calculated using the method of alchemical free energy perturbation (FEP)<sup>9</sup>. The two end states of a transformation with Hamiltonian  $H_1$  (in water: with coupling with the solvent) and  $H_0$  (in the vacuum: without coupling with the solvent) are coupled by a parameter  $\lambda$ ,

$$H(\lambda) = \lambda H_1 + (1 - \lambda)H_0 \quad (1)$$

The free energy difference  $\Delta G$  between both states can be estimated using discrete values of  $\lambda$ ,

$$\Delta G = \int_0^1 \left( \frac{\partial H(\lambda)}{\partial \lambda} \right)_{\lambda} d\lambda \quad (2)$$

For each system, 20 separate simulations with 20 different  $\lambda$  values. Two separate set of  $\lambda$  values were used: the first set of 10  $\lambda$  values to modify the LJ interactions between the solute and its environment and the second set of  $\lambda$  values to modify the solute charges. The non-linear soft-core scheme was adopted to compute the solute-solvent interactions in the free energy calculations to avoid end-point catastrophe and numerical issue. The method of MBAR<sup>10</sup> was used to compute free energy differences between different states.

Solvent accessible surface area (SASA) was calculated via a Connolly surface<sup>11</sup> generated with a probe radius of 1.4 Å using the GROMACS software<sup>6</sup>.

The proximal radial distribution function  $\rho G(r)$  was computed to present the normalized water concentration around a solute by referring to the bulk water density<sup>12,13</sup>. In  $\rho G(r)$ ,  $r$  is the minimum distance of a water oxygen atom to the pTMAO brush surface's atoms.

### Statistics

All measurements are represented as mean  $\pm$  standard deviation. The two-tailed student t-test was used to assess statistical differences between a pair of groups. Multiple comparisons were performed using one-way ANOVA followed by Tukey post hoc test. Significant difference was assumed at  $P < 0.05$ .

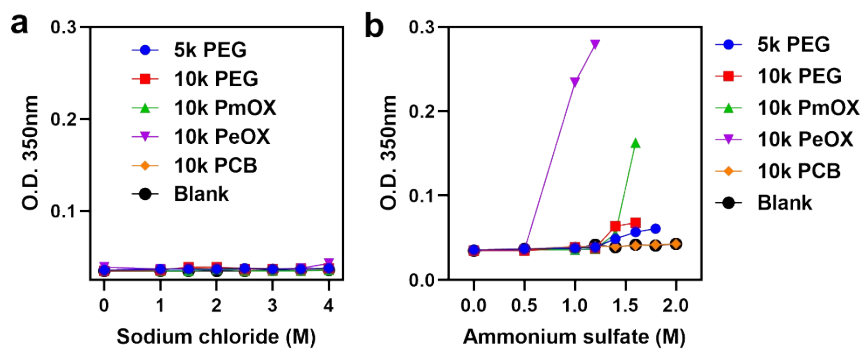


Figure S1. (a) Polymer solubility in NaCl solution (0-4M); (b) Polymer solubility in AS solution (0-2M);

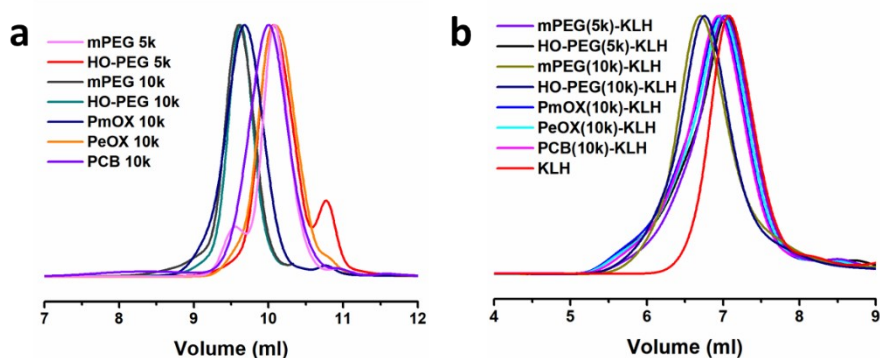


Figure S2. Size distribution of polymers (a) and polymer-KLH conjugates (b) measured by SEC.

Table S1. Composition of polymer-KLH conjugates (per KLH monomer)

Sample name	Molecular Weight(kDa)	Polymer chains
KLH	390	-
mPEG(5k)-KLH	412-430	4.5-8
HO-PEG(5k)-KLH	411-423	4.2-6.6
mPEG(10k)-KLH	442-462	5.2-7.2
HO-PEG(10k)-KLH	440-459	5.0-6.9
PmOX(10k)-KLH	436-465	4.6-7.5
PeOX(10k)-KLH	438-458	4.8-6.8
PCB(10k)-KLH	449-466	5.9-7.6

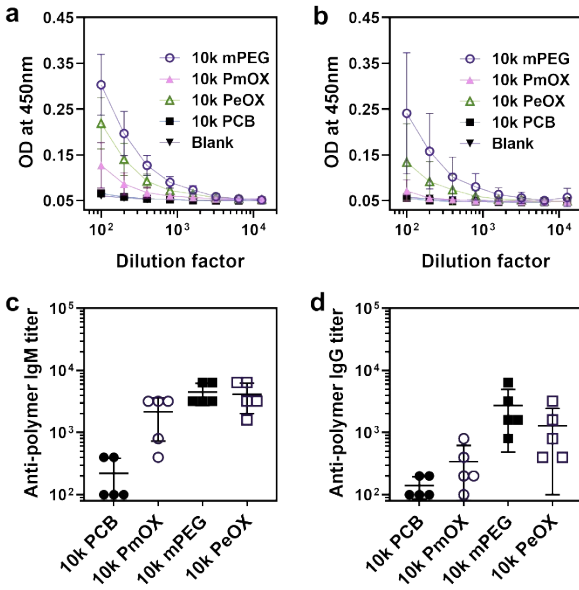


Figure S3. Anti-polymer Ab dilution profile of (a) IgM and (b) IgG elicited by polymer-KLH conjugates as determined by ELISA. Different polymers with same molecular weight (10k Da) were compared here. Anti-polymer IgM (c) and IgG (d) titers were plotted with increasing hydrophobicity from left to right.

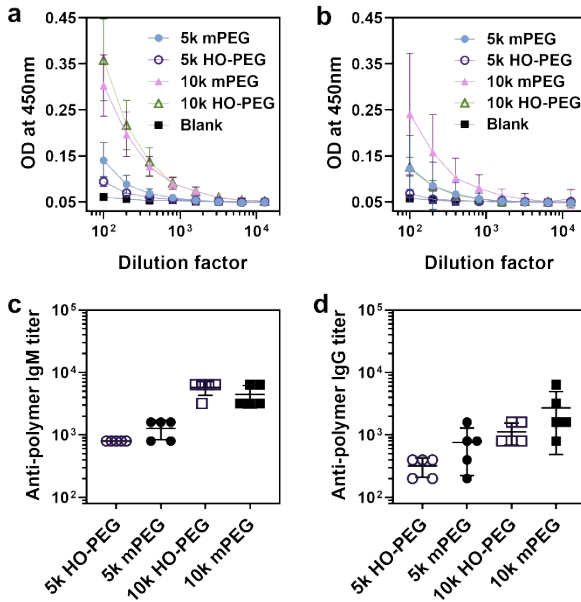


Figure S4. Anti-polymer serum dilution profile of (a) IgM and (b) IgG elicited by PEG-KLH conjugates. Influence of terminal group and molecular weight were evaluated here. Anti-PEG IgM (c) and IgG (d) titers were plotted with increasing PEG hydrophobicity from left to right.

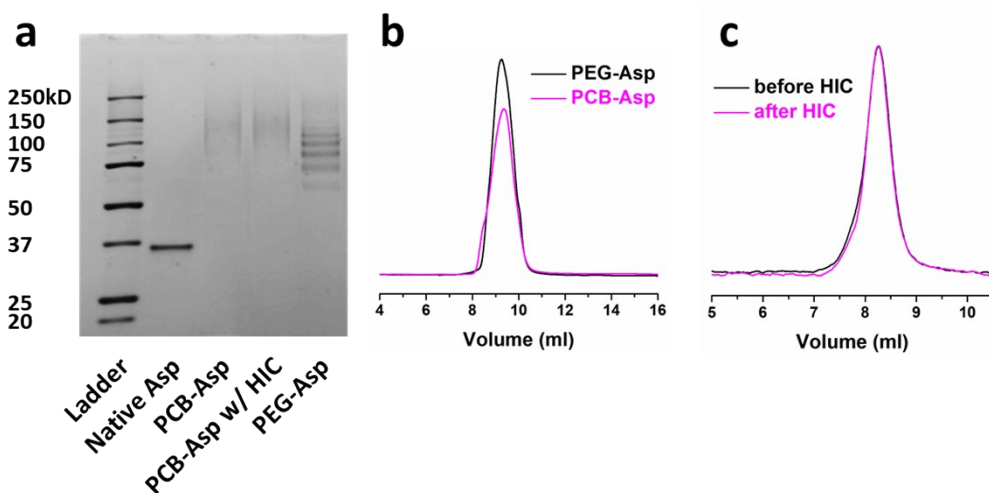


Figure S5. (a) SDS-PAGE image of Asp and Asp conjugates. Lanes from left to right represent protein standard, native Asp, PCB-Asp, PCB-Asp after HIC treatment and PEG-Asp; (b) SEC curves of PEG-Asp and PCB-Asp conjugate, recorded on a preparative FPLC system (column, Superdex 200 increase 10/300 gl); (c) SEC curves of PCB-Asp conjugate before and after HIC purification, recorded on an analytical GPC system (column, Ultrahydrogel 1000).

Table S2. Composition of Asp and Asp-polymer conjugates (per Asp monomer)

Sample name	Molecular Weight(kDa) by SDS-PAGE	Polymer chains by SDS-PAGE	Polymer chains by SEC <sup>a)</sup>	Normalized Asp activity (%) <sup>b)</sup>
Native Asp	35	-	-	100
5k PEG-Asp	72-110	7.4-15	10.2	45.7
10k PCB-Asp before HIC	120-150	8.5-11.5	9.1	43.2
10k PCB-Asp after HIC	120-150	8.5-11.5	9.3	44.1

<sup>a)</sup>, Polymer density on Asp conjugates was measured by SEC-MALS and calculated by Astra 7.0.

<sup>b)</sup>, Asp activities were measured by an asparaginase activity assay kit and normalized to unconjugated Asp.

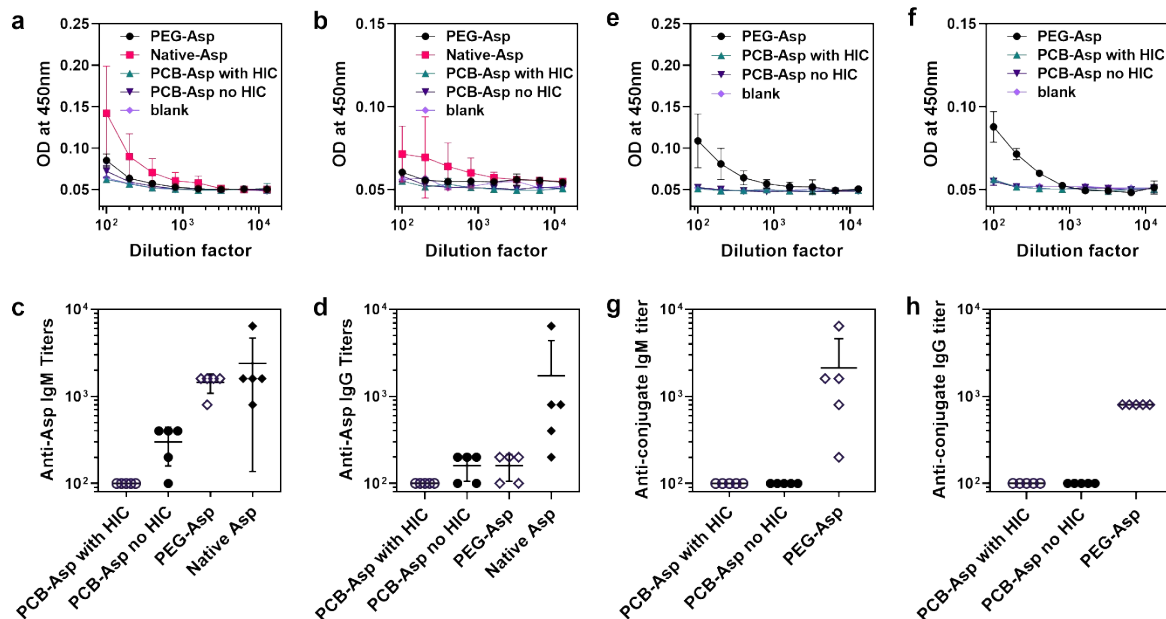


Figure S6. ELISA experiments determining Ab induction by Asp and Asp-conjugates. Three weekly doses of native Asp or polymer-Asp conjugates with and without HIC purification were S.C. administered to C57BL/6J mice (n=5). Serum was collected on Day 28 for ELISA test. Serum dilution profiles of anti-Asp IgM (a) and IgG (b) were used to assess Ab titers. The resulting anti-Asp IgM (c) and IgG (d) titers are plotted with increasing hydrophobicity from left to right. Serum dilution profiles of (e) IgM and (f) IgG elicited against whole conjugates. Anti-Asp conjugate IgM (g) and IgG (h) titers are plotted with increasing hydrophobicity from left to right.

## Reference

- (1) Li, B.; Yuan, Z.; Hung, H. C.; Ma, J.; Jain, P.; Tsao, C.; Xie, J.; Zhang, P.; Lin, X.; Wu, K., Revealing the immunogenic risk of polymers. *Angew. Chem. Int. Ed.* **2018**, *57* (42), 13873-13876.
- (2) Aida, Y.; Pabst, M. J., Removal of endotoxin from protein solutions by phase separation using triton x-114. *J. Immunol. Methods* **1990**, *132* (2), 191-195.
- (3) Application note 28-9964-9949 AA, High-throughput screening of HIC media in PreDictor™ plates for capturing recombinant Green Fluorescent Protein from E. coli (2011). GE Healthcare Bio-Sciences AB.
- (4) Li, B.; Yuan, Z.; He, Y.; Hung, H.-C.; Jiang, S., Zwitterionic nanoconjugate enables safe and efficient lymphatic drug delivery. *Nano Lett.* **2020**, *20* (6), 4693-4699.
- (5) a) T. K. Kishimoto, J. D. Ferrari, R. A. LaMothe, P. N. Kolte, A. P. Griset, C. O'Neil, V. Chan, E. Browning, A. Chalishazar, W. Kuhlman, F.-n. Fu, N. Viseux, D. H. Altreuter, L. Johnston, R. A. Maldonado, *Nat. Nanotechnol.* **2016**, *11*, 890-899; b) Y. Qi, A. Simakova, N. J. Ganson, X. Li, K. M. Luginbuhl, I. Ozer, W. Liu, M. S. Hershfield, K. Matyjaszewski, A. Chilkoti, *Nat. Biomed. Eng.* **2016**, *1*, 0002; c) B. A. Newman, E. A. Kabat, *J. Immunol.* **1985**, *135*, 1220-1231.
- (6) Abraham, M. J.; Murtola, T.; Schulz, R.; Páll, S.; Smith, J. C.; Hess, B.; Lindahl, E. GROMACS: High performance molecular simulations through multi-level parallelism from laptops to supercomputers. *SoftwareX* **2015**, *1*, 19-25.
- (7) Huang, J.; Rauscher, S.; Nawrocki, G.; Ran, T.; Feig, M.; De Groot, B. L.; Grubmüller, H.; MacKerell, A. D. CHARMM36m: an improved force field for folded and intrinsically disordered proteins. *Nat. Methods* **2017**, *14* (1), 71-73.
- (8) Essmann, U., Perera, L., Berkowitz, M.L., Darden, T., Lee, H. and Pedersen, L.G., A smooth particle mesh Ewald method. *J. Chem. Phys.* **1995**, *103*(19), 8577-8593.
- (9) Shirts MR, Mobley DL, Chodera JD. Alchemical free energy calculations: ready for prime time?. *Annu. Rep. Comput. Chem.* **2007**, *3*, 41-59.
- (10) Shirts, M.R. and Chodera, J.D. Statistically optimal analysis of samples from multiple equilibrium states. *J. Chem. Phys.* **2008**, *129* (12), 124105.

- (11) Eisenhaber, F., Lijnzaad, P., Argos, P., Sander, C., Scharf, M., The double cubic lattice method: efficient approaches to numerical integration of surface area and volume and to dot surface contouring of molecular assemblies. *J. Comput. Chem.*, **1995**, *16*(3), 273-284.
- (12) Huang, H., Zhang, C., Crisci, R., Lu, T., Hung, H.C., Sajib, M.S.J., Sarker, P., Ma, J., Wei, T., Jiang, S., Chen, Z., 2021. Strong surface hydration and salt resistant mechanism of a new nonfouling zwitterionic polymer based on protein stabilizer TMAO. *J. Am. Chem. Soc.*, 2021,*143*(40), 16786-16795.
- (13) Sarker, P., Chen, G., Sajib, M.S.J., Jones, N.W., Wei, T., 2022. Hydration and Antibiofouling of TMAO-derived Zwitterionic Polymers Surfaces Studied with Atomistic Molecular Dynamics Simulations. *Colloids Surf. A Physicochem. Eng.*, **2022**, *653*, 129943.